第16回性能に基づく橋梁等の耐震設計に関する
シンポジウム講演論文集（2013年7月）

Evaluation on Effect by Bearing Modeling for a RC Column based on E-Defense Excitation

Zhongqi SHI[1] ・ Kenji KOSA[2] ・ Tatsuo SASAKI[3]

[1]Student Member of JSCE, Ph.D. Candidate, Graduate School of Engineering, Kyusyu Institute of Technology
(〒804-8550 Sensui-cho 1-1, Tobata-ku, Kitakyushu, Fukuoka)
[2]Member of JSCE, Ph.D., Professor, Department of Civil Engineering, Kyusyu Institute of Technology
(〒804-8550 Sensui-cho 1-1, Tobata-ku, Kitakyushu, Fukuoka)
[3]Member of JSCE, M.E., Manager, Technical Generalization Division, Nippon Engineering Consultants Co., Ltd.
(Currently in the doctoral program at Kyushu Institute of Technology)

1. INTRODUCTION

In 1995 Kobe Earthquake, a number of bridges collapsed because the RC columns which supported the decks of the bridges failed in flexure at the base. It is known that the main cause of the flexural failure at the base during Kobe Earthquake is the lack of flexural capacity as well as ductility capacity resulted from underestimated seismic lateral force, insufficient amount of ties and inadequate development of the lap-splice of ties. Almost all of the columns which failed in Kobe Earthquake were built in 1970s and designed based on the seismic coefficient method in accordance with 1964 Design Specifications of Steel Road Bridges, by Japan Road Association[1].

A number of the bridges built in 1970s were retrofitted after Kobe Earthquake. However, the bridges, which have similar properties with the column failed in Kobe Earthquake and do not retrofit, still exist. Therefore, it is important to investigate the failure mechanisms of the columns failure in Kobe Earthquake. As a consequence, the first shake table experiment using E-Defense was conducted in December 2007, for a large scale reinforced concrete column that represents typical columns built in the 1970s, namely C1-1[2]. The residual damage condition at base of column of C1-1 is shown in **Fig. 1**, from which we can observe extensive damage of covering concrete and several buckling of longitudinal reinforcing bars.

Study in this paper introduces the correlations on C1-1 between experimental test and analytical result. Study flow is illustrated in **Fig. 2**. Aiming at reappearing the damage of C1-1 based on dynamic analysis and verifying the possible influence by modeling of bearing system, especially the effect by the consideration of frictional coefficient of movable bearing on longitudinal direction, dynamic analysis with the frictional coefficient being 0.12 (average based on elemental experiment) is conducted and compared with experimental result. Further parameter study on frictional coefficient is performed in following chapters.

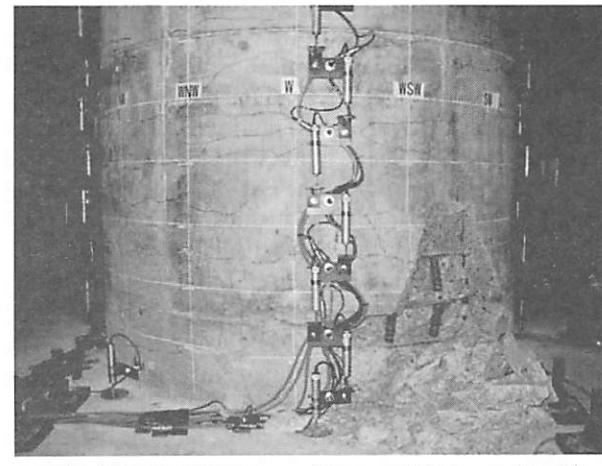

Fig. 1 Residual Damage at Bottom of Column after 1st Excitation of C1-1 (view from west side)

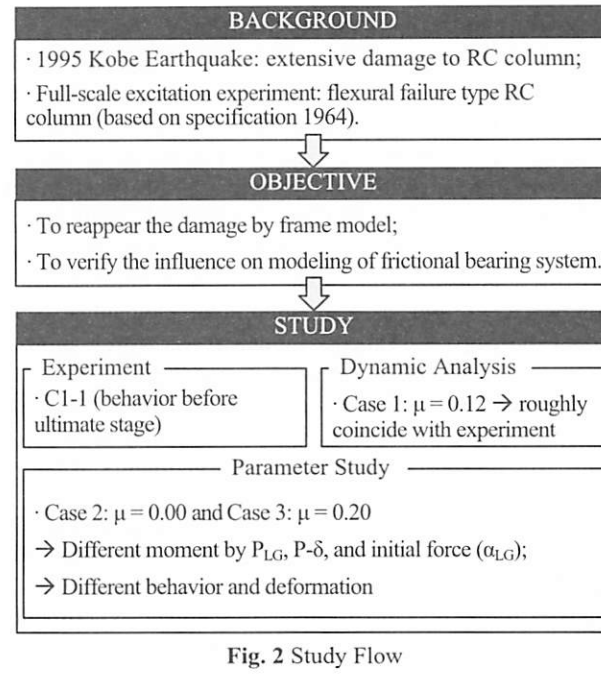

Fig. 2 Study Flow

2. EXPERIMENTAL SETUP AND ANALYTICAL CONDITION

As mentioned in Chapter 1, C1-1 is the specimen that was design to damage by flexural moment. In this chapter, condition of C1-1 specimen and experimental setup, as well as the analytical modeling with the frictional coefficient being 0.12 (average based on elemental experiment) will be explained in details.

(1) C1-1 Specimen and Experiment Setup

C1-1 is a 7.5m tall, 1.8m diameter reinforced concrete column as shown in **Fig. 3**. It was anchored to E-Defense shake table by a 1.8m thick square footing. It was designed as a full-scale model based on a combination of the static lateral force method and the working stress design (seismic coefficient method) which were specified in the 1964 Design Specifications of Steel Road Bridges[1]. As shown in **Fig. 3**, the column has 3 layers of longitudinal reinforcing bars with 29mm diameter, respectively 32, 32 and 16 at the outer, middle and inner layers. Deformed circular stirrups with 13mm diameter are provided at 300mm interval, except outer ties at the top 1.15m zone and at the base 0.95m zone where they are provided at 150mm interval. Stirrups are lap spliced with 390mm (30 times of its diameter). Consequently, the longitudinal reinforcement ratio is 2.02% and the tie volumetric reinforcement ratio is 0.32% for middle and 0.42% for top and base. On the day of experiment, actual strength of longitudinal bars, stirrups and concrete were measured as 366.0 MPa, 193.0 MPa and 33.0 MPa.

The seismic performance of C1-1 specimen in the longitudinal direction was evaluated based on the 2002 JRA Design Specification of Highway Bridges[3]. The yield displacement δ_y and ultimate displacement δ_u are 0.046m and 0.099m respectively.

Footing of C1-1 was fixed on shake table of E-Defense. The table was excited using E-Takatori ground motion. Main excitation using 100% E-Takatori ground motion was conducted twice.

(2) Analytical Modeling and Conditions

3D frame model is established for C1-1 specimen, for all column, decks and end supports as shown in **Fig. 4**. Trilinear M-Φ is assumed to the elements of column, while all other members are assumed as elastic elements. Stress-strain relationship of concrete, by Specification for Highway Bridges: Part III Concrete Bridge[4], is shown in **Fig. 5**. Actual strength measured on experiment day of 33.0 MPa is used. Consequently, M-Φ relationship for column can be got, as an example for element at base shown in **Fig. 6**. Takeda model is used for un-/re-loading hysteresis for column element. It should be noticed that to perform the analysis, M-Φ curve beyond ultimate stage is assumed to be the extending from yield stage. As a result, current analysis is mainly used to discuss the behavior before the ultimate stage.

Bearing system is idealized as illustrated in **Fig. 7**. Bilinear frictional spring is utilized in longitudinal for movable bearing. Because average frictional coefficient μ is got as 0.119 by velocity tests in element experiments of this bearing, as shown in **Fig. 8**, 0.12 is used for

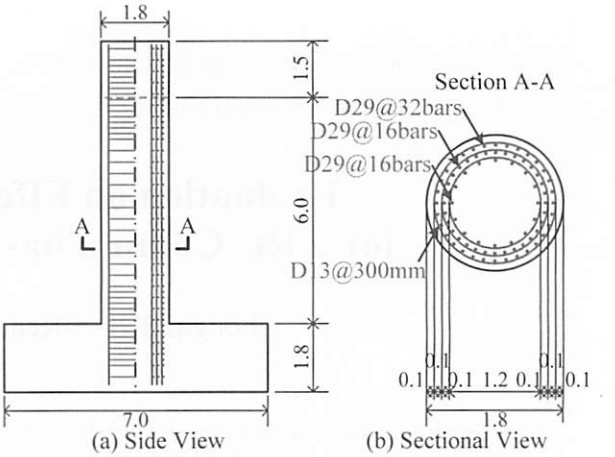

Fig. 3 C1-1 Column on E-Defense

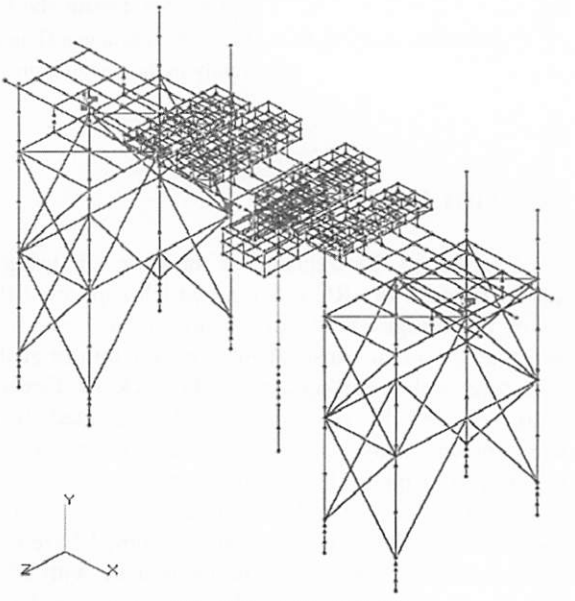

Fig. 4 Analytical Model

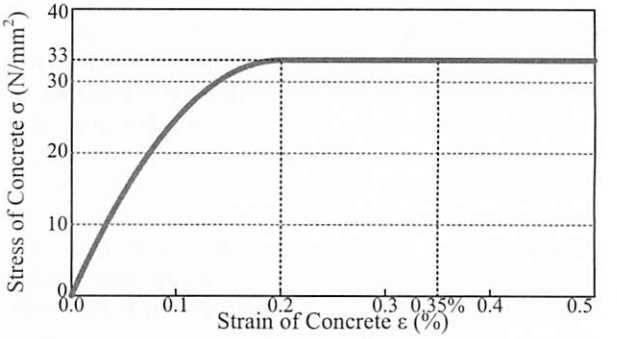

Fig. 5 σ-ε of Concrete

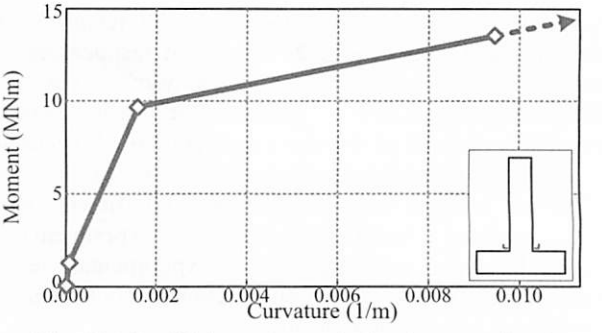

Fig. 7 M-Φ of Column (example for element at base)

standard model. Impact springs are used for contact and separation at side sliders. Besides, Rayleigh damping, considering modal damping ratio of 0.1 % was assumed at 1Hz and 25Hz, since the radiational energy dissipation of a column anchored to a shake table is extremely smaller than real energy dissipation of a column embedded in the ground[5]. Response acceleration at the base of column which was evaluated by averaging the measured accelerations on shake table at four corners is input to the base of footing by assuming the footing is rigid. Wave forms on longitudinal direction and transversal direction are shown in **Fig. 9**. It can be found that peak acceleration of -8.22 m/s^2 and 5.76 m/s^2 occurred at 6.62s and 4.00s for each direction. Time interval of analysis is 1/1000 s.

3. ANALYTICAL RESULT OF STANDARD CASE

As being explained formerly, 100% E-Takatori ground motion was applied to C1-1 specimen twice. However, extensive damage already occurred to the column in the 1st excitation. As the strain histories of longitudinal bars at 0.3m from base during the 1st excitation shown in **Fig. 9**, we can see that first yield of longitudinal bar occurred at 4.58s and 4.11s for SW side and NE side respectively. Furthermore, longitudinal bar on SW side (**Fig. 10** (a)) suffered notable compressive strain from 6.63s, with the peak strain exceeding 15,000μ. On the opposite side, longitudinal bar on NE side (**Fig. 10** (b)) experienced significant tensile strain, maximum about 20,000μ at 6.70s. On the other hand, as the response displacement histories shown in **Fig. 11**, top on column had already moved over 0.099m (δ_u mentioned in Section 2.1) on longitudinal direction in the experiment (black solid line shown in **Fig. 11** (a)). It can be inferred that the base of column has reached ultimate stage around 6.63s ~ 6.70s in the experimental test. Consequently, our current analytical result is mainly used to explain the phenomenon of column before 6.6s. Further discussion is necessary for the reasonability and reappearance after 6.6s (beyond the ultimate stage).

(1) Response Displacement

Response displacement histories on top of column (7.5m from base of column) are shown in **Fig. 10** for the longitudinal direction (**Fig. 11** (a)) and the transversal direction (**Fig. 11** (b)), comparing the results by experiment and analysis.

Divided by the time point of 6.6s, we can see that response displacements in analysis are considerably close to experimental result until 6.6s. In details, peak displacements before 6.6s are compared in **Table. 1**. It can be observed that the peak value has finite error on longitudinal direction (+1.2% and -3.9%), while obvious error (+22.2% and +11.1%) occurred on transversal direction. Thus, the analysis roughly reappears the response displacement in experiment until 6.6s although agreement on transversal direction is not sufficiently high.

On the other hand, after 6.6s, computed displacement in analysis shows the displacement shifted towards positive compared with the experimental result, although

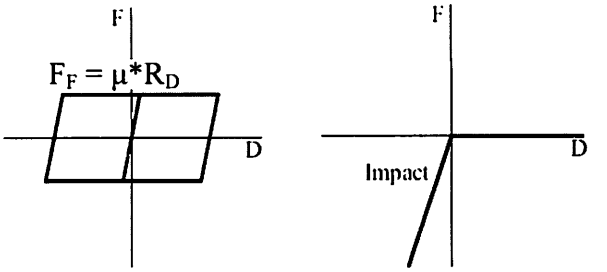

(a) Movable Bearing (b) Side Slider

Fig. 7 Modeling of Bearings

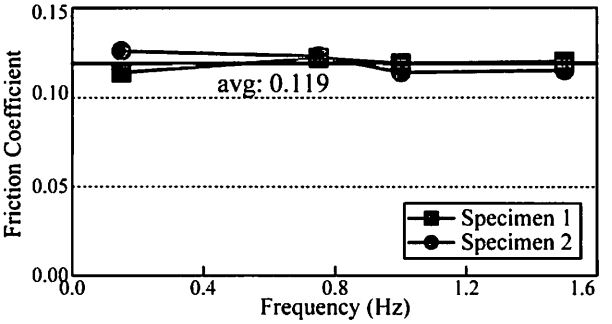

Fig. 8 Result of Element Experiments on Frictional Coefficient of Movable Bearings (effect of velocity)

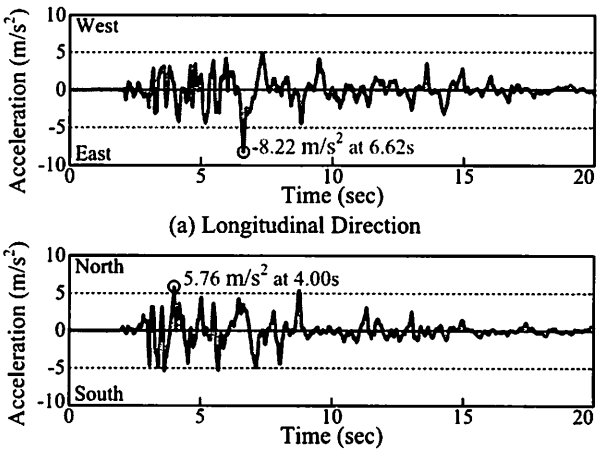

(a) Longitudinal Direction

(b) Transversal Direction

Fig. 9 Input Wave Forms

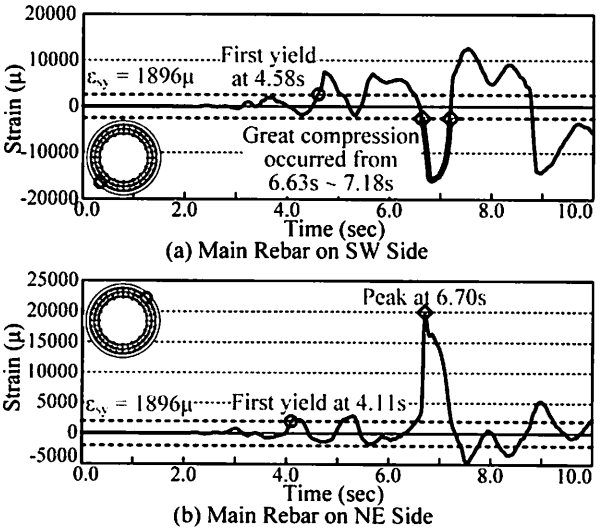

(a) Main Rebar on SW Side

(b) Main Rebar on NE Side

Fig. 10 Strain History of Longitudinal Bar during the 1st Excitation (at 0.3m from base)

the trends of response displacement histories are similar. The unaccurately evaluated M-Φ relationship after the ultimate stage and Takeda model un-/re-loading hysteresis possibly caused these obviously errors.

(2) M-δ Histories

As mentioned formerly, first yield of longitudinal bars occurred after 4.1s and ultimate stage occurred around 6.6s. Thus, M-δ histories are illustrated separately in **Fig. 12** from 0.0s to 4.1s (before the first yield), and in **Fig. 13** from 4.1s to 6.6s (after the first yield). Here, the moment at section of column base and the displacement on top of column (7.5m from base) are plotted.

As the response M-δ histories before the first yield (from 0.0s to 4.1s) shown in **Fig. 12**, we can see that the computed results are very close to the experimental results, with almost same displacement although slightly smaller flexural moment in analysis on negative side, for both that around transversal direction in **Fig. 12** (a) and that around longitudinal direction in **Fig. 12** (b). This suggests that experiment of C1-1 specimen is well reappeared by our frame model before the first yield of longitudinal reinforcing bars with acceptable accuracy.

On the other hand, after the first yield (from 4.1s to 6.6s), analytical result roughly coincides with experimental result around transversal direction (when deck moves in longitudinal direction) as shown in **Fig. 13** (a), while smaller flexural moment but greater displacement is got in analysis around longitudinal

Table. 1 Comparison of Peak Displacement before 6.6s

Displacement (m)		Experiment	Analysis	
			Disp	Error
LG	+	0.0724	0.0733	+1.2%
	-	-0.0463	-0.0445	-3.9%
TR	+	0.0715	0.0874	+22.2%
	-	-0.0945	-0.1050	+11.1%

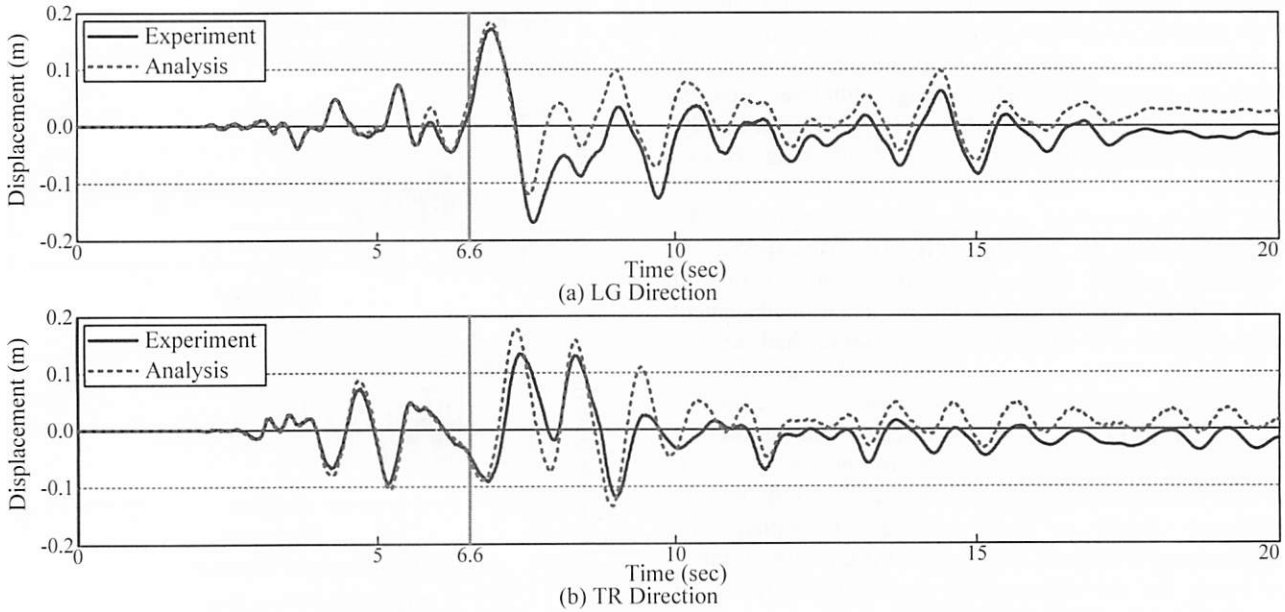

Fig. 11 Comparison of Response Displacement Histories on Top of Column during the 1st Excitation

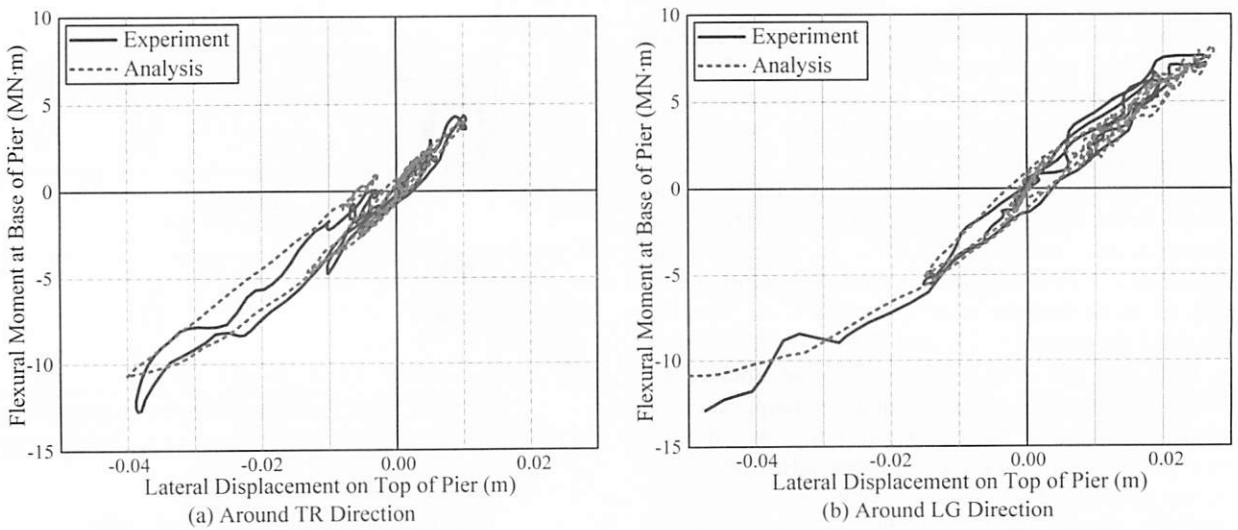

Fig. 12 Comparison of Response M-δ Histories Before First Yield (0.00s ~ 4.10s) during the 1st Excitation

direction (when deck moves in transversal direction) as shown in **Fig. 13** (b). From the un-/re-loading loops in both figures, we can see that loops by analysis show greater displacement corresponding to particular moment, which suggests that un-/re-loading hysteresis might not be accurately evaluated beyond the yield stage.

(3) Response Curvature

Furthermore, analytical correlation is evaluated based on response curvature as well. Comparisons of the curvature distribution at 5.355s (when top of column suffers maximum displacement on longitudinal direction during 0.0s ~ 6.6s), and the response curvature histories are shown in **Fig. 14** and **Fig. 15** respectively. Curvatures around transversal direction (when deck moves on longitudinal direction) are plotted as representative.

For the curvature distribution along height of column from base as shown in **Fig. 14**, it can be found that analytical result provides a very smooth curve of curvature distribution, with its general trend similar to that by experimental test. However, at height of 0.04m from base, the experiment shows curvature significantly greater than that by analysis. Attention should be paid that the pull-out effect of longitudinal reinforcing bars is not taken into consideration in current analysis. This is probably the main reason of the smaller curvature at 0.04m of column from base. For the heights of 0.18m, 0.58m and 0.98m from base, analytical results are notably greater than experimental results, while for heights of 0.38m and 0.78m, analytical results are only slightly smaller than experimental results.

To confirm them in details, the curvature around transversal direction at heights of 0.18m and 0.38m from base are shown in **Fig. 15** as examples. We can see that curvature history at 0.38m (shown in **Fig. 15** (a)) in analysis roughly coincides with experimental result before 6.6s, although after 6.6s the analysis fails to reappear great residual curvature which occurred in experimental test. Besides, at 0.18m from base (shown in **Fig. 15** (b)), curvature is obviously smaller in experiment than in analysis. Uneven distribution of curvature in experiment possibly caused this. Furthermore, for the curvature distribution of both heights, noticeable residual curvature could be observed in experimental test, which are not simulated accurately by current Takeda model.

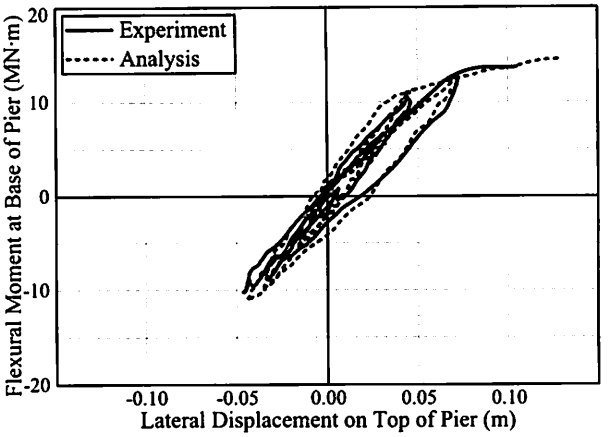

(a) Around TR Direction

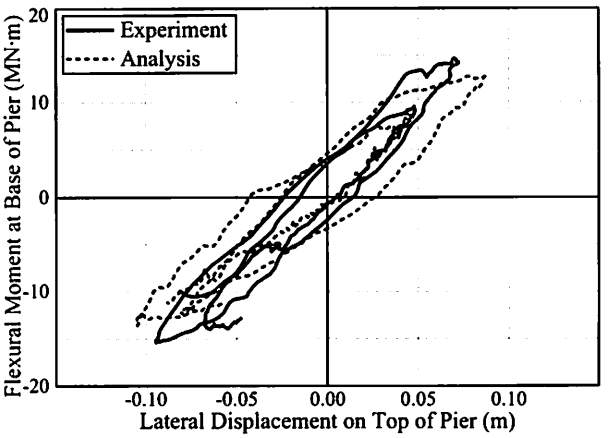

(b) Around LG Direction

Fig. 13 Comparison of Response M-δ Histories After First Yield (4.10s ~ 6.60s) during the 1st Excitation

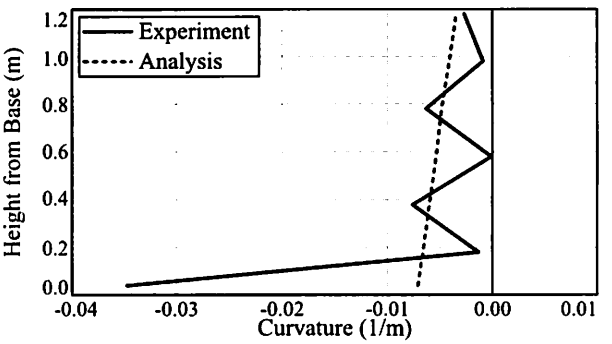

Fig. 14 Comparison of Curvature Distribution along Height of Column from Base at 5.355s

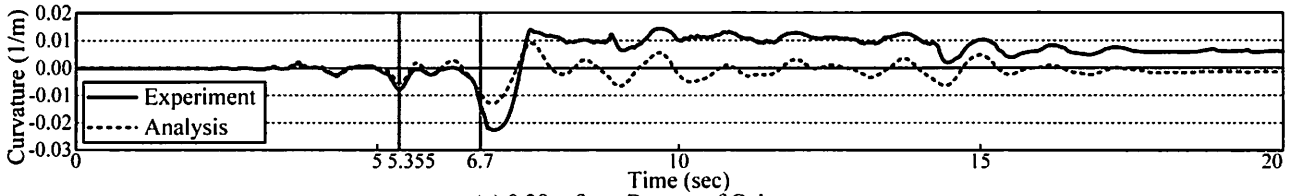

(a) 0.38m from Bottom of Column

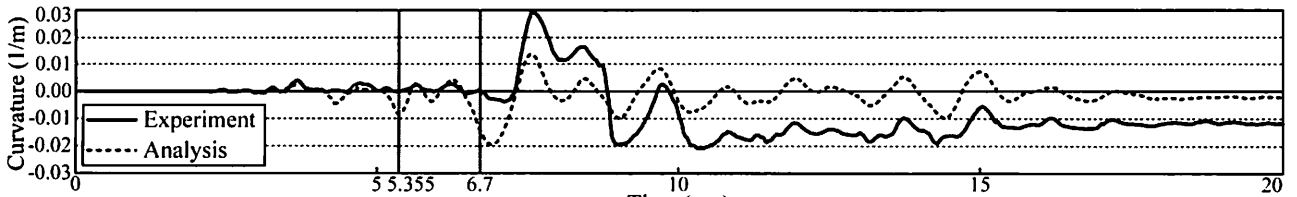

(b) 0.18m from Bottom of Column

Fig. 15 Comparison of Response Curvature Histories during the 1st Excitation (around TR direction)

(4) Friction of Movable Bearing on End Supporters

As being explained in Section 2.2, average friction coefficient (μ=0.12) is used in standard analysis, according to the result of element experiment for movable bearing. In the analysis, response P-δ history is plotted in **Fig. 16** (the movable on west end supporter is shown here as representative). From the figure it can be understood that the movable bearing begins to slide on longitudinal direction at as early as 2.16s. This indicates that in standard case of analysis (with friction coefficient μ being 0.12), the movable bearing does not resist greatly on longitudinal direction. Especially after the first yield (4.1s ~ 6.6s), notable horizontal displacement occurs with limited resistance from this bearing.

To sum it up, based on the dynamic analysis of standard case (μ=0.12), the response displacement on top of column (height of 7.5m from base), and the moment acting on base of column were approximately reappeared for the experimental test until 6.6s, although there is still particular error for the curvature distribution along column. Thus, the flexural behavior of this column was roughly simulated based on standard case.

4. EVALUATION ON EFFECT OF FRICTION OF MOVABLE BEARINGS

As the result of standard case (μ=0.12) explained in Chapter 3, the flexural behavior of column in the experimental test was roughly reappeared. In this chapter, the effect of friction by movable bearings will be discussed, by evaluating the response displacement on top of column, the flexural moment at base of column.

(1) Analytical Cases on Friction of Movable Bearings

As being explained in Section 2.2, series of element experiments were conducted for confirming the frictional coefficient of movable bearing on end supports on the longitudinal direction. Based on these experiments,

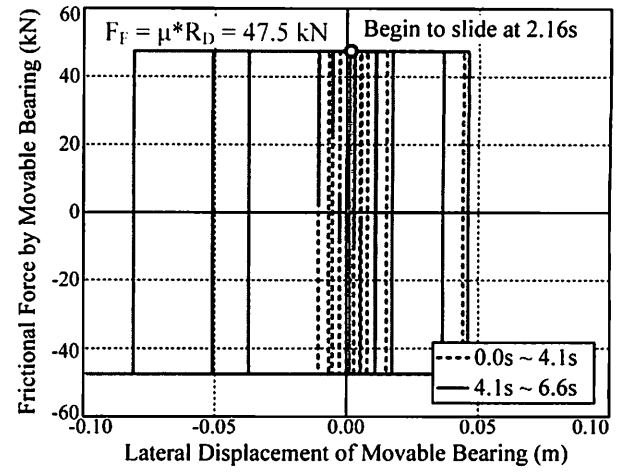

Fig. 16 Response P-δ History of Movable Bearing during the 1st Excitation

Table. 2 Analytical Cases

Cases	μ	Evidence
Case 1	0.12	Average of element experiment
Case 2	0.00	Perfect free assumption by specification
Case 3	0.20	Further experiment for other specimens

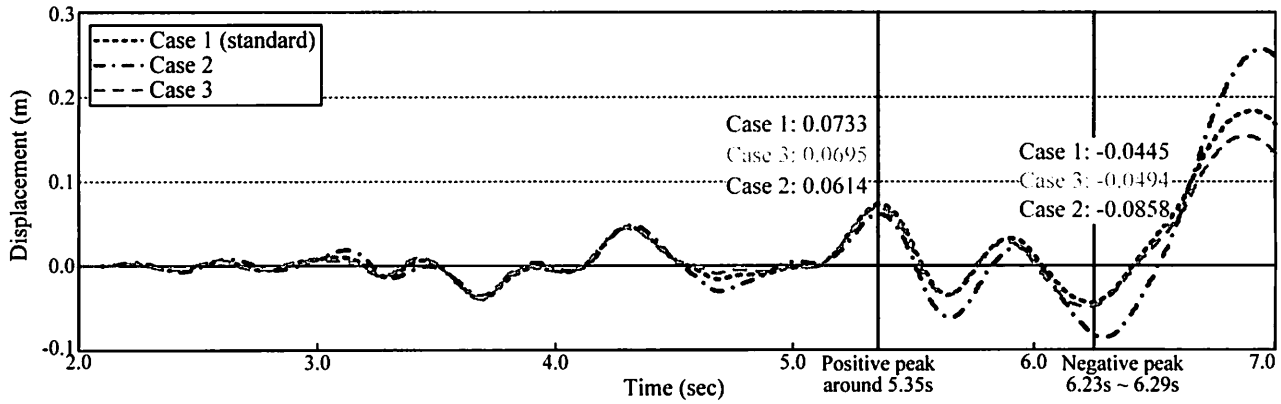

Fig. 17 Response Displacement History on Top of Column in Longitudinal Direction

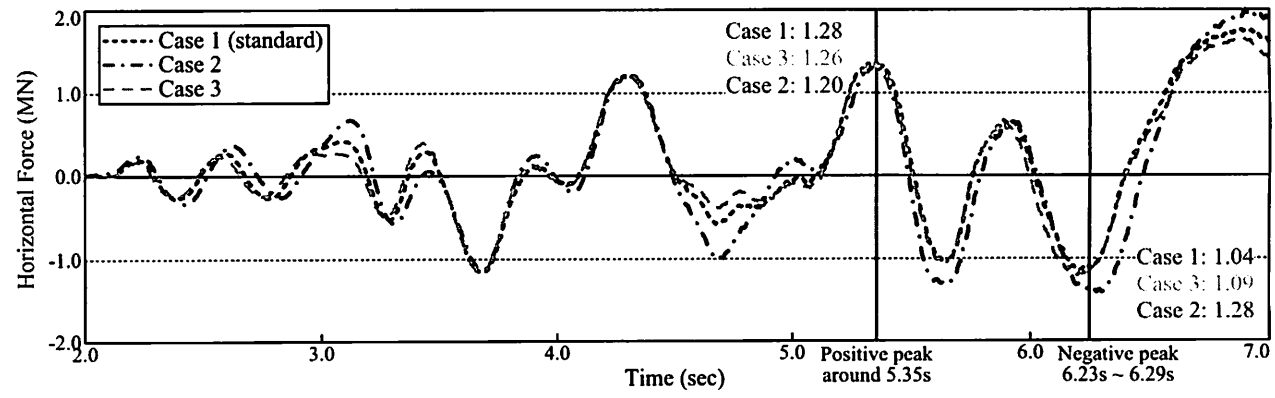

Fig. 18 Horizontal Force Histories on Top of Column in Longitudinal Direction

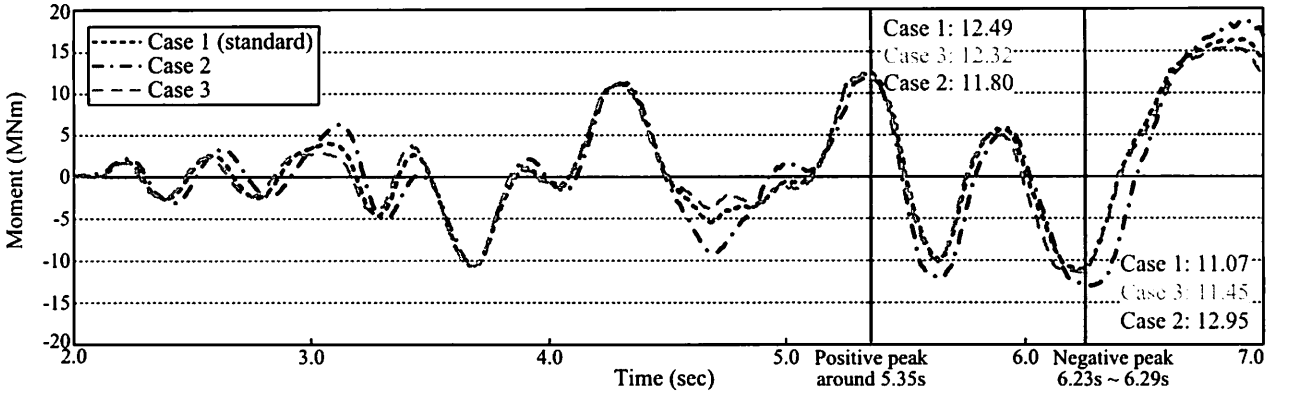

Fig. 19 Moment (around TR direction) Histories at Base of Column

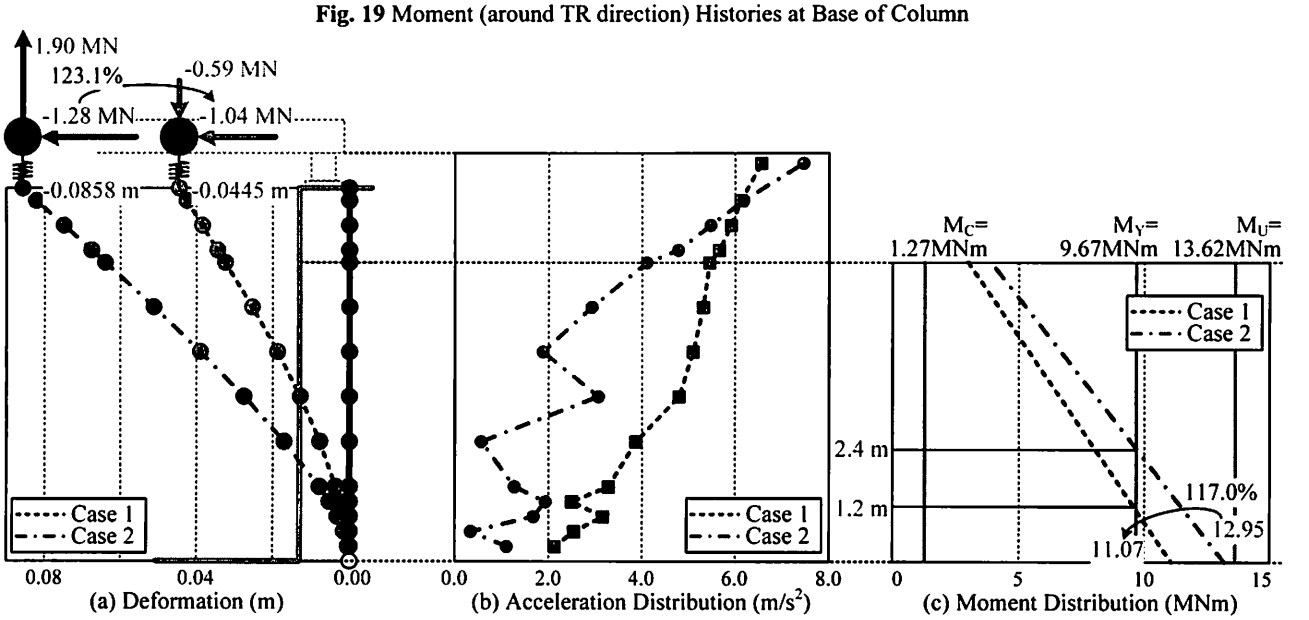

Fig. 21 Comparison of Peak Responses between Case 1 (at 6.24s) and Case 2 (at 6.29s)

frictional coefficient was assumed as 0.12 as the average value in Case 1 (standard case), illustrated in **Table. 2**. On the other hand, according to Japanese Specification[3], friction is suggested to be ignored in design procedure for movable bearing. Therefore, frictional coefficient μ is set as 0.00 in Case 2, as perfectly free. Besides, based on further tests in this series experiment on bridge, about 0.20 frictional coefficient was observed, which was greater than the average value based on element tests. This was considered to be caused by multi-surface-friction induced by transversal movement of deck. Consequently, frictional coefficient μ is assumed as 0.20 in Case 3, for better understanding the actual effect by friction of movable bearing on the behavior of column.

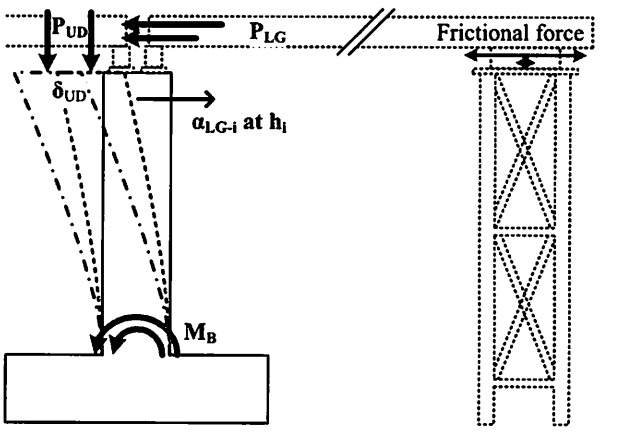

Fig. 20 Mechanism of Different Moment at Base

(2) Results and Evaluations

Comparison on response histories (0.0s ~ 7.0s) of the displacement on top of column (7.5m from base), the longitudinal force from superstructure, and the flexural moment at base of column, is shown in **Fig. 17 ~ Fig. 19** respectively. It can be found that Case 2 (no friction) has notably greater response than Case 1 (μ=0.12), while the difference of result between Case 3 (μ=0.20) and Case 1 is slight. In details, peak responses are compared. Peaks are reached at 5.355s, 5.360s and 5.350s in Case 1~3 respectively on positive side, and at 6.240s, 6.290s and 6.230s on negative side. The negative peak is the greatest before 6.6s. For positive peaks, response of Case 1 is greatest of 0.0733m displacement, 1.28 MN longitudinal force on top, and 12.49 MN·m moment at base. Case 2 (no friction) provides smaller result of 0.0614m displacement, 1.20 MN longitudinal force, and 11.80 MN·m moment at base, which is respectively 83.8%, 98.4% and 98.6% of Case 1. Besides, result of Case 3 (μ=0.20) is slightly smaller than Case 1 with 94.8%

displacement (0.0695m), 98.4% force (1.26 MN) and 98.6% moment (11.80 MN·m). For negative peaks, on the other hand, Case 2 gives greatest response without friction of -0.0858m displacement, -1.28 MN force, and -12.95 MN·m moment at base, respectively 192.8%, 123.1% and 117.0% of Case 1. Result of Case 3 (μ=0.20) is similar Case 1, as well as positive peaks, with 111.0% displacement (-0.0494m), 103.4% force (-1.09 MN) and 105.2% moment (-11.45 MN·m).

To verify different moment at base, mechanism is shown in **Fig. 20** and expressed by Eq. (1) for Case 1 & 2:

$$M_B = M_{LG} + M_{UD} + M_\alpha = P_{LG} \times h - P_{UD} \times \delta_{LG} - \Sigma(\alpha_{LG\text{-}i} \times m_i \times h_i) \quad (1)$$

Here, notations are explained in **Fig. 20**.

It is known that moment is contributed by three parts: by longitudinal force (P_{LG}), by P-δ effect (by P_{UD} and δ_{LG}) and by distributed inertial force along column (in terms of α_{LG}). With no friction, column may take greater P_{LG}, although P_{LG} and α_{LG} may not be clear between cases. Thus, difference of longitudinal force may affect the moment and displacement mostly.

Specific force and displacement conditions are shown in **Fig. 21** ((a) for deformation and forces, (b) for acceleration distribution, (c) for moment distribution). It can be found that P_{LG} is 23.1% greater in Case 2 than in Case 1, while P_{UD} provides negative moment in Case 2. In **Fig. 21** (b), acceleration in Case 2 is smaller than in Case 1 for column except the beam upon it. To discuss effect of every aspect, contribution ratio is calculated and illustrated in **Fig. 22**. It indicates that P_{LG} contributes mostly (69.1% in Case 1 and 76.9% in Case 2), the effect by P-δ effect can be ignored (0.2% and -1.2%), although distributed inertial force along column gives particularly notable effect (respectively 30.7% and 24.3%). Moment distribution is shown in **Fig. 21** (c), from which we can see M_B increases to 12.95 MN·m in Case 2 (117.0% of 11.07 MN·m in Case 1. Furthermore, due to generally noticeable moment, the range that reaches yield stage is 2.4m from base in Case 2. This is about twice of that in Case 1 (1.2m). These 17.0% greater moment at base and twice height beyond yield stage are considered as the main reasons for significant displacement on column top in Case 2 (-0.0858m, 192.8% of -0.0445m in Case 1).

Consequently, peak responses until 6.6s were got around 6.23s ~ 6.29s. Greater difference occurred with or without friction (192.8% displacement in Case 2 as shown in **Fig. 23**), by comparing Case 1 and Case 2. But the result by μ=0.20 (Case 3) had only slight difference (3.4% for moment, 7.2% for longitudinal force and 11.0% for displacement) with that by μ=0.12 (Case 1).

5. CONCULSIONS

Based on the dynamic analyses for C1-1 specimen, and the discussion of effect by friction on end supporters, following conclusions have been drawn:

(1) By standard case (μ=0.12), response of column in experiment was roughly reappeared before the ultimate stage. Displacement and moment were calculated with acceptable accuracy, while calculated curvature did not coincide well with experiment, especially for the base of column. Ignoring of bar pull-out effect might cause this error of curvature.

(2) By parametric study on frictional coefficient, notable response was got when the friction was ignored. Due to 23% greater longitudinal force from superstructure, about 17% greater moment at base occurred, as well as twice high of yield zone at base of column. These greater longitudinal force, moment at base and higher yield zone led to more significant displacement.

(3) On the other hand, by the analyses with frictional coefficient μ=0.12 or μ=0.20, the response were relatively similar to each other. Peak of moment, longitudinal force and displacement varied slightly about 3.4%, 7.2% and 11.0% respectively.

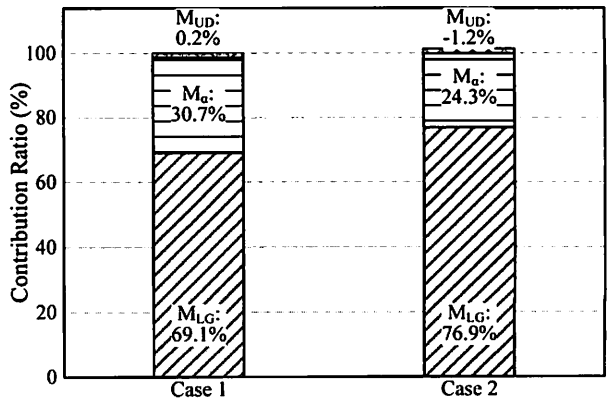

Fig. 22 Contribution Ratio for Moment for Negative Peak

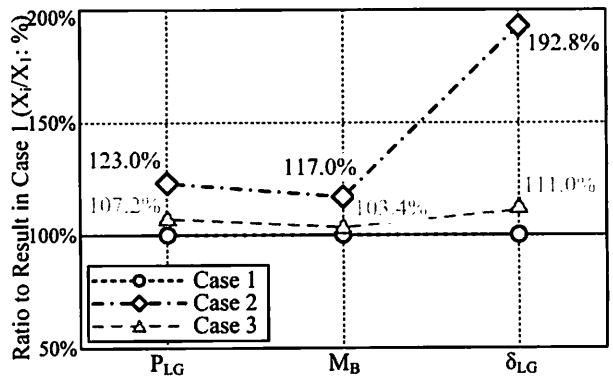

Fig. 23 Effect by Friction Coefficients on Peak Responses

Reference

1) Japan Road Association: Design *Specification of Steel Highway Bridges*, 1964.

2) Ukon, H., et. al.: Large-scale Shake Table Experiment on a Component Model (C1-1 model) Using E-Defense, *Technical Note of The National Research Institute for Earthquake Science and Disaster Prevention*, No.331, 2009.

3) Japan Road Association: *Specification for Highway Bridges: Part V Seismic Design*, 2002.

4) Japan Road Association: *Specification for Highway Bridges: Part III Concrete Bridges*, 2002.

5) Sakai, J. and Unjoh, S.: Earthquake Simulation Test of Circular Reinforced Concrete Bridge Column under Multidirectional Seismic Excitation, *Earthquake Eng. and Engineering Vibration*, Vol.5, No.1, pp. 103-110, 2006.